Antiviral CD8+ T Cell Responses in Neonatal Mice: Susceptibility to Polyoma Virus–induced Tumors Is Associated with Lack of Cytotoxic Function by Viral Antigen–specific T Cells

By Janice M. Moser,* John D. Altman,‡§ and Aron E. Lukacher*

*From the *Department of Pathology, the ‡Department of Microbiology and Immunology, and the §Emory Vaccine Center, Emory University School of Medicine, Atlanta, Georgia 30322*

Abstract

Polyoma virus is a potent oncogenic pathogen when inoculated into newborn mice of particular H-2^k strains. Using D^k tetramers containing the dominant antipolyoma CD8+ T cell epitope, middle T protein (MT)389–397, and intracellular interferon γ staining, we enumerated MT389-specific CD8+ T cells in infected neonates having opposite susceptibilities to polyoma virus–induced tumors. In resistant mice, MT389-specific CD8+ T cells dramatically expanded during acute infection in neonates to a frequency rivaling that in adults; furthermore, in both neonatal and adult mice, this antipolyoma CD8+ T cell response exhibited nearly identical T cell receptor (TCR) functional avidities and TCR functional fingerprints. Susceptible mice mounted an MT389-specific CD8+ T cell response of only fourfold lower magnitude than resistant mice; but, in clear contrast to resistant mice, these CD8+ T cells lacked ex vivo MT389-specific cytotoxic activity. However, MT389-specific CD8+ T cells in resistant and susceptible mice expressed similar TCR avidities, perforin levels, and surface type O-glycan levels indicative of mature CD8+ T cell effectors. Upon in vitro restimulation with infected antigen-presenting cells, CD8+ T cells from acutely infected susceptible neonates acquired strong MT389-specific cytotoxicity. These findings indicate that polyoma-specific CD8+ T cells are armed with, but restrained from deploying, their cytotoxic effector function in mice susceptible to polyoma virus tumorigenesis.

Key words: CD8+ T lymphocytes • intracellular IFN-γ • neonatal mice • polyoma virus • tetramers

Introduction

Recent studies have called into question the long-held concept that neonatal lymphocytes are inherently prone to induction of tolerance (1–3). Newborn mice inoculated by certain viruses are capable of generating antiviral CD8+ CTLs (3, 4). In addition, several studies have shown that neonatal DNA vaccination efficiently primes antigen-specific CD8+ T cell responses and CD4+ T cell–dependent antibody responses that are long-lived and protect against virus challenge (5–8). A common feature of nearly all studies of neonatal T cell responses in vivo, however, is that antigen-specific T cell responses are examined in adulthood, not during the neonatal period. In particular, no direct information is available about the magnitude and functionality of antigen-specific T cell responses during neonatal life.

Polyoma virus is a potent oncogenic mouse pathogen when inoculated into newborn mice belonging to particular inbred strains (9, 10). An essential contribution of T cells in neonatal mice towards protection against polyoma virus–induced tumors was provided by early studies showing that neonatal thymectomy enhanced polyoma tumor susceptibility of otherwise resistant mice (11, 12). High susceptibility to polyoma virus tumorigenesis is a property of a subset of H-2^k mouse strains (9). We recently found that the H-2^k MHC and the endogenous mouse mammary tumor provirus, *Mtv*-7, are major codeterminants of susceptibility to polyoma virus–induced tumors (10). This susceptibility is imparted by the *Mtv*-7–encoded superantigen that, by negatively selecting thymocytes bearing particular Vβ domains, depletes the peripheral T cell pool in H-2^k mice of polyoma-specific CD8+ T cell precursors, most of which express Mtv-7 superantigen-reactive Vβ domains (10). Using polyoma virus–specific CTL cloned

Address correspondence to A.E. Lukacher, Dept. of Pathology, Woodruff Memorial Research Building, 1639 Pierce Dr., Atlanta, GA 30322. Phone: 404-727-1896; Fax: 404-727-5764; E-mail: alukach@emory.edu

lines isolated from neonatally infected tumor-resistant H-2^k mice, we identified the immunodominant polyoma-specific CTL epitope as a D^k-restricted 9-amino acid peptide derived from the viral middle T (MT)[1] oncoprotein, designated MT389–397 (13). Interestingly, limiting dilution analysis revealed that susceptible mice are not entirely devoid of MT389-specific CTLs but possess 10–20-fold fewer CTL precursors directed to this epitope than mice resistant to polyoma virus tumorigenesis (13). The presence of these antigen-specific CD8$^+$ T cells in mice prone to develop polyoma tumors is highly reminiscent of the frequent observation that tumor-specific CD8$^+$ T cells are detected in the peripheral T cell repertoire of cancer patients (14–16). A central question, then, is why antipolyoma CD8$^+$ T cells in susceptible mice fail to control the outgrowth of polyoma virus–induced tumors.

Using D^k tetramers containing the MT389–397 peptide, in conjunction with MT389 peptide-triggered intracellular IFN-γ production, we visualized dramatic expansion of antigen-specific CD8$^+$ T cells during acute polyoma infection in adult mice (17). This MT389-specific CD8$^+$ T cell expansion was associated with the appearance of strong ex vivo antigen-specific cytotoxic activity and clearance of infectious polyoma virus. In this study, we applied these single cell analyses to enumerate the MT389-specific CD8$^+$ T cell responses in polyoma virus–infected neonatal mice and assess their effector functionality directly ex vivo. We found that tumor-resistant neonatal mice mount a vigorous, cytotoxic and cytokine effector function-competent, CD8$^+$ T cell response against polyoma virus infection that rivals that of mice infected in adulthood. In contrast to the difference in MT389-specific CTL precursor frequency determined by limiting dilution analysis, direct ex vivo analyses revealed that MT389-specific CD8$^+$ T cells attain a peak expansion in tumor-susceptible mice only fourfold lower than that of resistant mice. Although these antipolyoma CD8$^+$ T cells in susceptible mice retain full capacity to produce IFN-γ, they lack ex vivo cytotoxic effector activity. This effector function deficit by antigen-specific CD8$^+$ T cells likely compromises host defense against polyoma virus tumorigenesis.

Materials and Methods

Animals. C3H/HeNCr and CBA/JCr mice were purchased from the Frederick Cancer Research and Development Center of the National Cancer Institute. All protocols for animal studies were approved by the Institutional Animal Care and Use Committee of Emory University. Pregnant mice were housed in individual microisolator cages and monitored daily for births. Adult mice were used at 6–9 wk of age.

Virus and Virus Inoculation. Wild-type polyoma virus, strain A2, was molecularly cloned and plaque purified, and virus stocks were prepared on primary baby mouse kidney cells, as described (13). Adult mice were inoculated subcutaneously in hind foot-

pads with 2 × 10^6 PFU of virus. Newborn mice were inoculated subcutaneously in hind footpads with 2 × 10^5 PFU of virus within 12 h of birth.

Cell Lines. AG104A cells (18) were maintained in DMEM containing 5% FCS (Mediatech, Inc.). BALB/3T3 clone A31 cells were obtained from the American Type Culture Collection and maintained in DMEM containing 5% bovine calf serum (Summit Biotechnology).

Synthetic Peptides. Peptides were synthesized by the solid-phase method on a Symphony/Multiplex Peptide Synthesizer (Rainin) with F-moc chemistries. HPLC analysis showed that peptides were >90% pure. The following peptides were used in this study: MT389–397 (RRLGRTLLL) and a panel of alanine monosubstituted MT389–397 analogue peptides. Peptides were diluted in 10% serum-containing medium immediately before use.

Polyoma Virus Plaque Assay. Spleens were snap-frozen in sterile Kontes tubes (Kontes Glass Company), adjusted to 50 mg/ml in DMEM at 4°C, and homogenized using an overhead stirrer (Wheaton) and disposable Teflon pestles (Kontes). Homogenized tissues were freeze–thawed three times, incubated for 45 min at 42°C, and centrifuged to remove cell debris. Supernatants were titered for infectious virus by plaque assay on BALB/3T3 clone A31 cells as described (17). The detection limit for this plaque assay is 1 PFU/mg spleen.

^{51}Cr Release Assay. Peptide-pulsed ^{51}Cr-labeled AG104A (H-2^k, class II MHC–negative) target cells were prepared as described (13), and aliquoted at 5,000 cells/well into U-bottom 96-well microtiter plates (Costar). Single cell suspensions of spleens were treated with RBC lysing buffer (Sigma-Aldrich), and viable mononuclear cells aliquoted at the indicated E/T ratios. After a 5-h incubation at 37°C, half the volume of each well was removed and counted in a 1470 Wallac Wizard gamma counter.

Values for percent specific lysis were calculated as described (17). Spontaneous ^{51}Cr release from target cells in all assays was <15% of total ^{51}Cr release. Percent specific lysis values represent mean values of quadruplicate wells. SEMs were always <5% of the mean values and are omitted.

Flow Cytometry. Single cell suspensions of spleen were prepared, RBCs lysed, and 10^6 cells stained in phenol red–free RPMI 1640 (Life Technologies) containing 2% FCS and 0.1% sodium azide (FACS® buffer) for 1 h at 4°C, followed by three washes in FACS® buffer and fixation in PBS containing 1% paraformaldehyde. Cells were surface-stained with PE- or Tricolor-conjugated rat anti–mouse CD8α mAb (clone CT-CD8a; Caltag) and FITC-conjugated rat anti–mouse CD11a, CD43 (1B11), or α/β TCR mAbs (BD PharMingen), and allophycocyanin-conjugated D^k/MT389 tetramers. H-2D^k tetramers containing the MT389–397 peptide or the gag88–96 peptide (RRKGKYTGL), a retroviral CTL epitope (19), were prepared and their specificity verified as described (17, 20). Samples were acquired on a FACSCalibur™ (Becton Dickinson), and data analyzed using CELLQuest™ (Becton Dickinson) and FlowJo software (Tree Star, Inc.). Plots are gated on CD8$^+$ T cells and values shown are the percentages of CD8$^+$ T cells in the indicated quadrant. Of necessity, different litters of neonatally inoculated mice were used for each of the time points for the kinetic analyses of MT389-specific CD8$^+$ T cell responses (see Figs. 2 and 5); therefore, gates for each postinfection time point were individually assigned based on analysis of CD8$^+$ T cells from uninfected mice.

For FACS® sorting, RBC-lysed spleen cells were stained in phenol red–free RPMI 1640 plus 2% FCS (FACS®-sorting buffer) containing PE-conjugated anti-CD8α, FITC-conjugated

---

[1]*Abbreviations used in this paper:* ELISPOT, enzyme-linked immunospot; MT, middle T protein.

anti–α/β TCR, and allophycocyanin-conjugated D[k]/MT389 tetramers for 1 h at 4°C. Cells were washed and resuspended in FACS®-sorting buffer, then sorted on a FACS Vantage™ (Becton Dickinson).

Intracellular IFN-γ and Perforin Staining. RBC-lysed spleen cells were cultured for 5 h in 96-well flat-bottom microtiter plates (Costar) at 10^6 cells/well in 0.2 ml/well IMDM (Life Technologies) containing 10% FCS, 50 μM 2-ME, and penicillin/streptomycin, and supplemented with 1 μg/ml brefeldin A (Sigma-Aldrich), 50 U/ml human rIL-2 (BD PharMingen), and synthetic peptides at 10 μM. Cells were then surface stained with PE-conjugated rat anti–mouse CD8α mAb (Caltag) and allophycocyanin-conjugated D[k]/MT389 tetramers. After washing, cells were permeabilized and stained for intracellular IFN-γ with FITC-conjugated rat anti–mouse IFN-γ mAb (clone XMG1.2; BD PharMingen) or its isotype control Ab (rat IgG1; BD PharMingen) using the Cytofix/Cytoperm kit, according to the manufacturer's instructions (BD PharMingen).

For intracellular perforin staining, RBC-lysed spleen cells were surface stained with allophycocyanin-conjugated D[k]/MT389 tetramers for 30 min at 4°C. Cells were then fixed, permeabilized, and stained with rat anti–mouse perforin mAb (clone P1-8; Kamiya Biomedical Co.) or isotype-matched control Ab (rat IgG2a; Caltag), washed, then stained with PE-conjugated donkey anti–rat F(ab′)₂ IgG (Jackson ImmunoResearch Laboratories) using the FIX & PERM cell permeabilization kit, according to the manufacturer's instructions (Caltag). Finally, cells were stained with FITC-conjugated rat anti–mouse CD8α mAb (Caltag).

Single Cell Enzyme-linked Immunospot Assay for IFN-γ–secreting Cells. Pooled spleens from four newborn inoculated 13-d-old C3H/HeN mice were stained with anti-CD8α, anti–α/β TCR, and D[k]/MT389 tetramers and sorted by flow cytometry into three distinct populations, as described in Fig. 4. Each sorted population was serially diluted threefold in wells previously coated with rat anti–mouse IFN-γ, to which were then added 5×10^5 γ-irradiated (2,000 rad) syngeneic cells and MT389–397 peptide (0.1 μg/ml) or no peptide. After 36 h incubation at 37°C, single cell IFN-γ enzyme-linked immunospot (ELISPOT) assays were performed as described (21).

Results

Ex Vivo Polyoma-specific Cytotoxic Activity in Neonatally Infected Resistant Mice. Polyoma virus–specific CTL cloned lines are readily isolated from newborn inoculated mice of H-2[k] strains resistant to polyoma virus–induced tumors; these CTL lines are predominantly directed toward the D[k]-restricted MT389–397 epitope (13). Freshly explanted spleen cells from acutely infected adult C3H/HeN mice, a strain resistant to polyoma virus–induced tumors when inoculated at birth, exhibit high levels of MT389-specific cytotoxic activity (17). We asked whether MT389-specific CTL activity could be similarly detected ex vivo during acute infection in newborn inoculated C3H/HeN mice. As shown in Fig. 1 A, freshly explanted spleen cells from C3H/HeN mice inoculated at birth efficiently lysed MT389 peptide-coated syngeneic target cells. MT389-specific lysis was detected as early as day 8 of age, peaked at day 13 after infection, and was nearly undetectable by 3 wk of age (Fig. 1 A, and data not shown). Spleen cells from naive 13-d-old C3H/HeN mice did not lyse MT389-pulsed
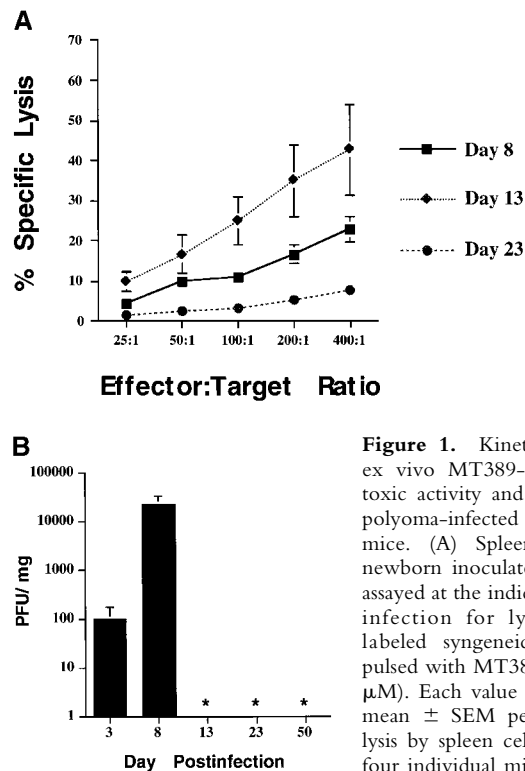

A

B

Figure 1. Kinetic analyses of ex vivo MT389-specific cytotoxic activity and virus titer in polyoma-infected C3H/HeN mice. (A) Spleen cells from newborn inoculated mice were assayed at the indicated day after infection for lysis of ^{51}Cr-labeled syngeneic target cells pulsed with MT389 peptide (10 μM). Each value represents the mean ± SEM percent specific lysis by spleen cells of three to four individual mice; results are representative of three experiments. No lysis of unpulsed target cells was seen by spleen cells from these infected mice at any postinfection time point, and spleen cells from naive neonatal and adult C3H/HeN mice did not lyse MT389 peptide-pulsed targets (reference 17, and data not shown). (B) Spleens from newborn inoculated mice of the indicated ages were harvested, homogenized, and titered for polyoma virus by plaque assay. Each value represents the mean ± SD PFU/mg spleen from five to six individual mice. *, below detection limit of 1 PFU/mg.

target cells (data not shown). The emergence of MT389-specific cytotoxicity in neonatal mice, as previously seen in adult infected mice (17), is associated with clearance of infectious polyoma virus (Fig. 1 B).

In Vivo Visualization of the MT389-specific CD8⁺ T Cell Response in Neonatal C3H/HeN Mice. Using D[k]/MT389 tetramers and intracellular staining for MT389-stimulated IFN-γ, we showed that adult C3H/HeN mice mount large-scale expansion of antigen-specific CD8⁺ T cells during acute polyoma virus infection (17). The potent ex vivo antipolyoma cytotoxic activity expressed by newborn infected C3H/HeN mice suggested that neonatal and adult mice mount similarly massive expansions of MT389-specific CD8⁺ T cells to polyoma virus infection. As shown in Fig. 2 A, by 8 d of age, newborn inoculated C3H/HeN mice generated a population of antigen-specific CD8⁺ T cells readily detected by D[k]/MT389 tetramers. By day 13 after infection, these tetramer⁺CD8⁺ T cell numbers had expanded to a point where they constituted nearly one-third of the CD8⁺ T cells in the spleen that expressed high levels of CD11a, a phenotype for antigen-experienced T cells. Even by day 50, in the absence of detectable infectious virus in the spleen, MT389-specific CD8⁺ T cells still represented nearly 20% of activated CD8⁺ T cells. The
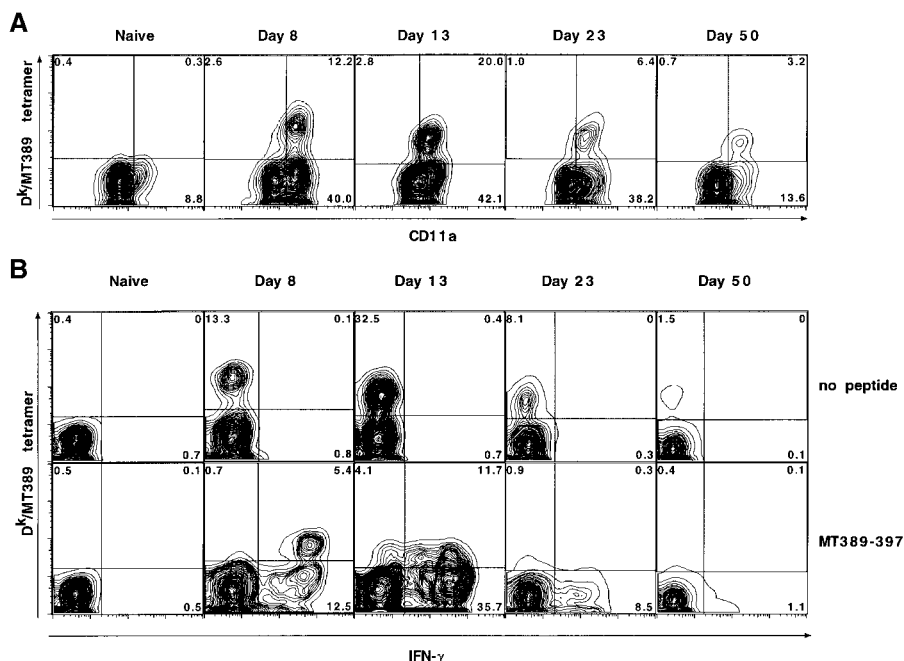
Figure 2. Visualization of MT389-specific tetramer+CD8+ T cells during polyoma infection in neonatal C3H/HeN mice. (A) Spleen cells from newborn inoculated mice at each of the indicated ages were stained with D^k/MT389 tetramers, and anti-CD8α and anti-CD11a mAbs, and analyzed by flow cytometry. Plots are gated on CD8+ T cells and values shown are the percentages of CD8+ T cells in the indicated quadrant. (B) Spleen cells from neonatally infected mice were cultured in the absence or presence of MT389 peptide (10 μM) for 5 h, surface-stained with D^k/MT389 tetramers and anti-CD8α, then stained for intracellular IFN-γ. FITC-conjugated isotype control Ab for the anti–IFN-γ mAb did not stain MT389 peptide-stimulated spleen cells from acutely infected neonatal C3H/HeN mice (data not shown). Plots are gated on CD8+ T cells and the values shown are the percentages of CD8+ T cells in the indicated quadrant. A naive 13-d-old C3H/HeN mouse is included as a specificity control. Plots are representative of three experiments using three to five mice per time point.

specificity of D^k/MT389 tetramers for spleen cells from acutely infected neonatal C3H/HeN mice was confirmed (a) by lack of staining by control D^k/gag88 tetramers, as previously shown in acutely infected adult C3H/HeN mice (17), and (b) by lack of D^k/MT389 tetramer staining when C3H/HeN neonates were inoculated with a replication-competent mutant polyoma virus carrying substitutions in the MT389–397 sequence that abrogate recognition by MT389-specific CD8+ T cells (data not shown).

Enumeration of MT389-specific CD8+ T cells in acutely infected neonatal mice by peptide-stimulated intracellular IFN-γ production revealed an unexpected discordance with D^k/MT389 tetramers in detecting antigen-specific CD8+ T cells. As shown in Fig. 2 B, at 8 and 13 d of age of newborn inoculated C3H/HeN mice, 25–30% more MT389-specific CD8+ T cells were detected by intracellu-

lar IFN-γ staining than by tetramer binding. Note that most of the IFN-γ+ CD8+ T cells show decreased tetramer staining as a result of ligand-induced TCR downmodulation. Interestingly, this quantitative discrepancy between tetramer and intracellular IFN-γ staining for antigen-specific CD8+ T cells resolves at time points after clearance of detectable infectious virus in the spleen. Because the MHC anchoring residues for peptides bound to D^k and K^k are distinct (P2 = basic residue for D^k, but acidic residue for K^k; references 13 and 22), it is highly unlikely that K^k presents the MT389–397 peptide to CD8+ T cells and is responsible for amplifying the number of IFN-γ+CD8+ T cells. Furthermore, spleen cells from acutely infected neonate and adult C3H/HeN mice lyse MT389 peptide-pulsed target cell lines of C3H.OL (K^dD^k), but not B10.A (K^kD^d), origin (references 13 and 23; data not shown).

Table I. *Comparison of MT389-specific CD8+ T Cells in Infected Neonate and Adult C3H/HeN Mice*

MT389-specific IFN-γ cells	Neonate				Adult			
	Day 8	Day 13	Day 23	Day 50	Day 5	Day 7	Day 12	Day 50
Total (×10⁶)	0.10 ± 0.02	1.39 ± 0.27	0.31 ± 0.03	0.14 ± 0.04	0.8 ± 0.09	3.81 ± 0.40	2.09 ± 0.17	1.06 ± 0.08
Percent CD8+ cells	20.2 ± 4.0	40.7 ± 2.9	6.8 ± 0.3	1.7 ± 0.3	8.2 ± 0.6	23.9 ± 1.8	15.2 ± 0.2	7.1 ± 0.6

Spleen cells from polyoma virus–inoculated mice at the indicated day after infection were stimulated with MT389 peptide for 5 h, then surface stained with PE-conjugated anti-CD8α, stained intracellularly with FITC-conjugated anti–IFN-γ, and analyzed by flow cytometry. No IFN-γ was produced by MT389 peptide–stimulated spleen cells from naive neonate and adult mice (data not shown). Values represent the mean ± SEM of gated CD8+ populations of three to six mice at each time point from three separate experiments.

As staining with D^k/MT389 tetramers underestimated the actual number of MT389-specific CD8$^+$ T cells in vivo in acutely infected neonatal mice, total numbers of MT389-specific CD8$^+$ T cells were determined by intracellular IFN-γ staining (Table I). Due to technical limitations associated with the very small number of T cells in the neonatal spleen, MT389-specific CD8$^+$ T cells could not be reliably detected under day 8 of age. However, even by day 8, one in five splenic CD8$^+$ T cells in newborn inoculated C3H/HeN mice was found to recognize the dominant MT epitope; this frequency matches that seen at the peak expansion of MT389-specific CD8$^+$ T cells during acute infection in adult C3H/HeN mice. Remarkably, by day 13 of age, ~40% of the splenic CD8$^+$ T cells in neonatal C3H/HeN mice recognize the MT389 epitope. The larger viral load during acute infection in neonates than in adults may promote this more vigorous expansion of antipolyoma CD8$^+$ T cells in newborn inoculated mice. Substantial numbers of MT389-specific CD8$^+$ T cells also persist in memory (day 50 after infection) in mice of both inoculation age groups, although differences in size between their respective antipolyoma memory CD8$^+$ T cell pools roughly correspond to differences in maximal expansion during acute infection.

Tetramer-negative Antigen-specific CD8$^+$ T Cells in Neonatally Infected Mice. Because low-affinity TCR show reduced levels of tetramer binding and faster tetramer dissociation rates (24, 25), we asked whether low TCR affinity accounted for the higher frequency of antigen-specific CD8$^+$ T cell effectors detected by intracellular IFN-γ staining than by tetramer binding in the infected neonatal mice. In acutely infected adult mice, enumeration of MT389-specific CD8$^+$ T cells by tetramer binding and peptide-induced intracellular IFN-γ production closely correspond (17). Therefore, the TCR avidity of adult versus neonate MT389-specific CD8$^+$ T cells was compared. Spleen cells from C3H/HeN mice at time point of peak ex vivo cytotoxic activity after newborn (day 13 after infection) and adult (day 8 after infection) virus inoculation were assayed for peptide dose dependence of target cell lysis. Because the spleens of neonate- and adult infected mice at these respective time points contain different numbers of MT389-specific CD8$^+$ T cells, the extent of target cell lysis at each peptide titration was normalized to equivalent numbers of MT389-specific CD8$^+$ T cells. As shown in Fig. 3 A, C3H/HeN mice inoculated at birth or as adults generated MT389-specific CTL effectors with virtually equivalent functional TCR avidity.

To explore whether MT389-specific CD8$^+$ T cells generated in infected adult and neonates differed in fine specificity for the MT389 epitope, we also compared the capacity of alanine monosubstituted MT389 analogue peptides to stimulate IFN-γ production by freshly explanted spleen cells from acutely infected neonate and adult C3H/HeN mice. We previously showed that each of these analogue peptides bound to purified D^k molecules with affinity equivalent to the wild-type peptide (20). As shown in Fig. 3 B, remarkably little variation in TCR functional finger-

prints was observed not only between individual mice of the same inoculation age group, but also between the neonatal and adult infected mice. In line with their similar fine specificity profiles, D^k/MT389 tetramer$^+$CD8$^+$ T cells in acutely infected neonatal C3H/HeN mice showed the same Vβ6- and Vβ8.1-dominated repertoire as adult C3H/HeN mice (reference 17, and data not shown).

We next asked whether subpopulations of MT389-specific CD8$^+$ T cells may be present in acutely infected neonatal mice that express TCRs at levels unfavorable for efficient tetramer binding, but sufficient to trigger T cell activation. Pooled spleen cells from 13-d-old newborn in-
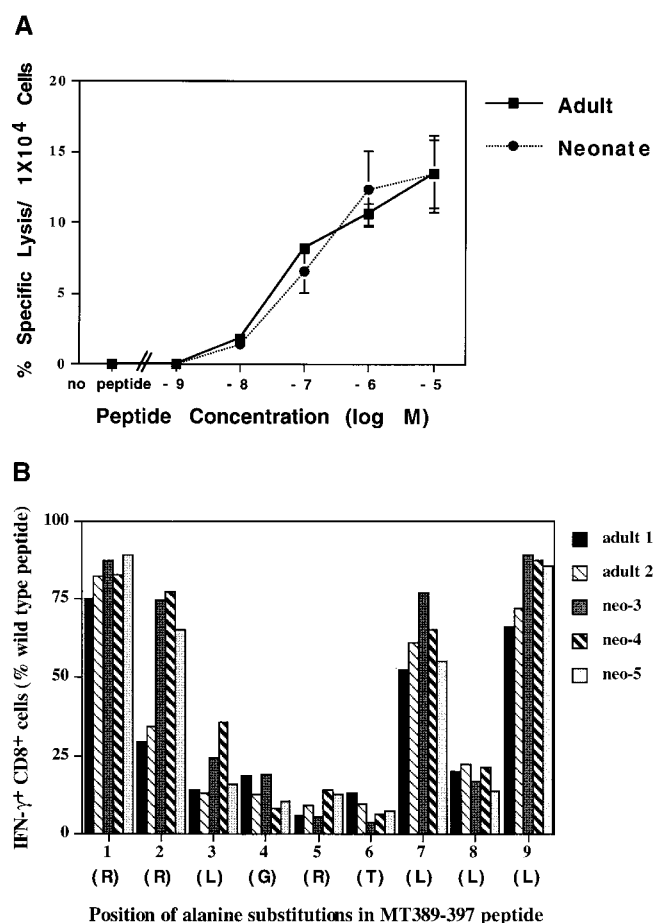

Figure 3. Comparison of TCR avidities and functional fingerprints of MT389-specific CD8$^+$ T cells from newborn and adult inoculated C3H/HeN mice. (A) Spleen cells from adult and neonatally infected mice at the peak of their antigen-specific CTL response (day 7 and day 13 after infection, respectively) were assayed in a ^{51}Cr release assay with syngeneic target cells pulsed with serial log dilutions of the MT389 peptide. Values represent the mean ± SEM percent specific lysis of three mice normalized to 10^4 antigen-specific CD8$^+$ cells, as determined by intracellular IFN-γ staining. (B) Spleen cells from day 7 and day 13 postinfection adult and neonatal mice, respectively, were stimulated for 5 h with wild-type MT389 peptide (10 μM) or with each of a panel of alanine monosubstituted MT389 peptides (10 μM), then stained for intracellular IFN-γ. The level of stimulation at each substituted peptide is presented as the percentage of the number of IFN-γ$^+$CD8$^+$ cells with respect to that seen with the wild-type peptide. Letters in parentheses indicate the amino acids at each of the positions in the wild-type peptide. Results are representative of three experiments.
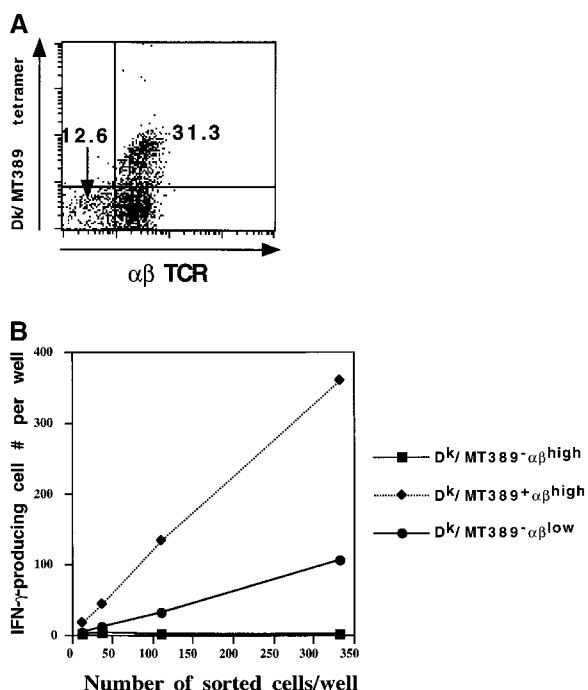
A

12.6 31.3

D^k/MT389 tetramer

αβ TCR

B

IFN-γ–producing cell # per well

■ D^k/ MT389⁻αβ^{high}
◆ D^k/ MT389⁺αβ^{high}
● D^k/ MT389⁻αβ^{low}

Number of sorted cells/well

Figure 4. TCR^{low} MT389-specific CD8$^+$ T cells in acutely infected neonatal mice. (A) Spleen cells from a 13-d-old newborn inoculated C3H/HeN mouse were stained with anti-CD8α, anti–α/β TCR, and D^k/MT389 tetramers directly ex vivo. The plot is gated on CD8$^+$ T cells and values shown are the percentages of CD8$^+$ T cells in the indicated quadrant. Plot is representative of six mice in two experiments. (B) Pooled spleen cells from four 13-d-old newborn inoculated C3H/HeN mice were stained as in A, and three CD8$^+$ T cell populations sorted as indicated. Each population was aliquoted in the presence of irradiated syngeneic unpulsed or MT389 peptide-pulsed feeder cells in an IFN-γ ELISPOT assay. In the absence of peptide, no IFN-γ–producing cells were detected in any of these FACS$^®$-sorted populations (data not shown).

oculated C3H/HeN mice were triple stained with D^k/ MT389 tetramers, anti-CD8α and anti–αβ TCR mAbs, and analyzed by flow cytometry. As shown in Fig. 4 A, there was a discrete population of tetramer$^-$CD8$^+$ T cells that had poor to absent α/β TCR expression. This α/β TCR$^{low/-}$ T cell population also expressed high levels of the activation marker CD11a (data not shown). To evaluate whether polyoma-specific CD8$^+$ T cells resided within this α/β TCR$^{low/-}$tetramer$^-$ population, three CD8$^+$ T

cells populations were FACS$^®$ sorted based on tetramer and α/β TCR expression, and MT389-specific cells then counted by IFN-γ ELISPOT assay. As shown in Fig 4 B, the sorted D^k/MT389 tetramer$^+$ population showed a near 1 to 1 correspondence between number of cells plated and the number of spots identified when stimulated with the MT389 peptide, whereas no MT389-stimulated IFN-γ secretion was detected by the α/β TCR$^+$tetramer$^-$ population. Interestingly, approximately one-third of the α/β TCR$^{low/-}$tetramer$^-$ cells contained MT389-specific CD8$^+$ T cells (Fig. 4 B).

MT389-specific CD8$^+$ T Cell Expansion in Neonatal Mice Susceptible to Polyoma Virus–induced Tumors. Because newborn inoculated H-2^k mice carrying the *Mtv-7* provirus are susceptible to polyoma virus–induced tumors (10), we applied tetramer and intracellular IFN-γ staining to attempt to visualize MT389-specific CD8$^+$ T cells in acutely infected neonatal mice of an H-2^k *Mtv-7$^+$* inbred strain, CBA/J. As shown in Fig. 5, both of these single cell methodologies detected antigen-specific CD8$^+$ T cells in infected CBA/J neonatal mice, but their frequency was clearly lower than in the neonatally infected resistant C3H/HeN mice at each of the same postinfection time points (Fig. 2 B). Like C3H/HeN infected neonates, maximal expansion of MT389-specific CD8$^+$ T cells was reached by 13 d of age in newborn inoculated CBA/J mice (Fig. 5, and data not shown). It is interesting to note that at this time point tetramer staining also accounts for only about two-thirds of the MT389 peptide-stimulated IFN-γ$^+$ CD8$^+$ T cells. Importantly, despite the opposite susceptibilities of these two inbred mouse strains, total splenic MT389-specific CD8$^+$ T cells in the resistant C3H/HeN neonates at day 13 after infection were only fourfold higher than in the infected susceptible CBA/J neonates at this age (Fig. 6).

CBA/J neonates were also considerably less efficient in eliminating infectious polyoma virus than C3H/HeN mice. Although splenic virus titers were equivalent at early stages of infection in neonatal mice of each strain, 8-d-old CBA/J mice possessed 10-fold higher levels of infectious virus in their spleens, with significant viral titers detected at least through day 23 after infection (Fig. 7). This higher peak and substantially longer sustained virus levels in neo-
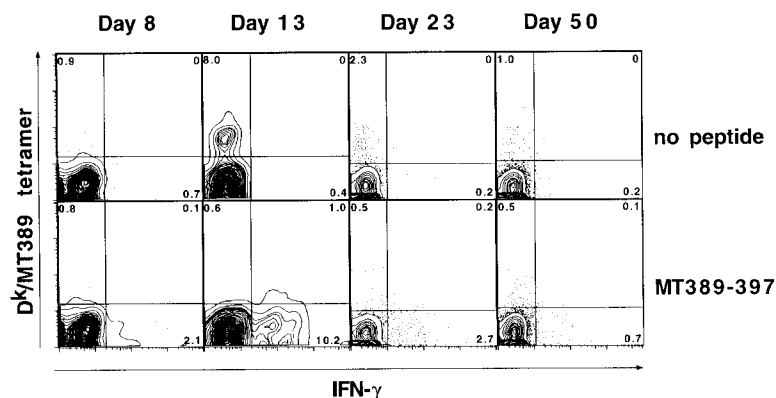
Day 8   Day 13   Day 23   Day 50

D^k/MT389 tetramer

IFN-γ

no peptide

MT389-397

Figure 5. Visualization of MT389-specific CD8$^+$ T cells in neonatally infected CBA/J mice by intracellular IFN-γ staining. Spleen cells from polyoma virus–infected neonatal mice were stained with D^k/MT389 tetramers and anti-CD8α mAb, followed by staining for intracellular IFN-γ. Plots are gated on CD8$^+$ T cells and the values shown are the percentages of CD8$^+$ T cells in the indicated quadrant. Plots are representative of three independent experiments using three to five mice per time point.
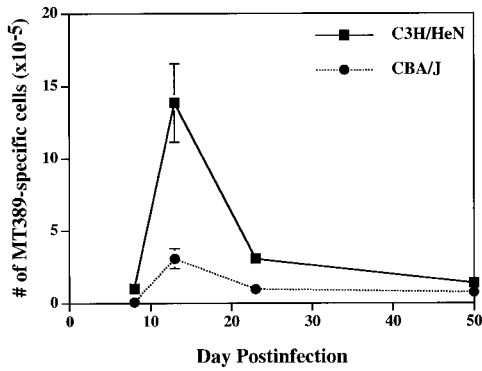
Figure 6. Comparison of the magnitude of MT389-specific CD8^{+} T cell responses by newborn inoculated C3H/HeN and CBA/J mice. Total numbers of splenic MT389-specific CD8^{+} T cells, as determined by intracellular IFN-γ staining, were determined for mice of each strain at the indicated ages. Values represent the mean ± SEM of three to five mice at each time point. Results are representative of two independent experiments.

natal CBA/J mice may, in fact, have also provided an antigenic stimulus to boost the size of the CBA/J memory CD8^{+} T cell pool, which was of nearly the same size as C3H/HeN neonates (Fig. 6).

Infected CBA/J Neonates Lack Ex Vivo MT389-specific Cytotoxic Activity. Although functionally competent to produce IFN-γ, we asked whether MT389-specific CD8^{+} T cells generated by newborn inoculated CBA/J mice also possess antigen-triggered cytotoxic activity. As shown in Fig. 8, freshly explanted spleen cells from acutely infected CBA/J neonates exhibited no detectable lysis against MT389 peptide-pulsed syngeneic target cells. The trivial explanation that expansion of MT389-specific CD8^{+} T cells was insufficient to permit detection of ex vivo target lysis is highly unlikely because, even at 13 d of age, CBA/J neonatal spleens contained slightly more MT389-specific CD8^{+} T cells (5,856 ± 60 cells/well at E:T = 400:1) than those of 8-d-old infected C3H/HeN mice (4,040 ± 120 cells/well at E:T = 400:1), which exhibit significant antigen-specific cytotoxicity (Fig. 1 A). Furthermore, competition between infected cells in the CBA/J neonate spleen and ^{51}Cr-labeled targets for CTL effectors is ruled out because spleen cells from 13-d-old newborn infected CBA/J mice (~2,500 PFU/mg spleen) did not inhibit MT389-specific ex vivo CTL activity by day 8–infected adult C3H/HeN mice (data not shown). That polyoma-infected
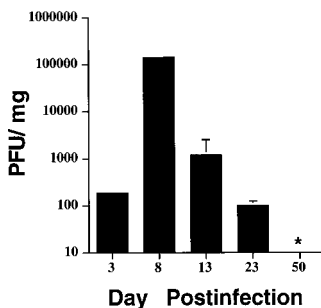
CBA/J mice are not inherently defective in generating ex vivo MT389-specific cytotoxic activity is illustrated by the capacity of spleen cells from acutely infected adult CBA/J mice to lyse MT389 peptide-loaded target cells. Importantly, the defect in ex vivo cytotoxic effector function by MT389-specific CD8^{+} T cells in acutely infected CBA/J neonatal mice is reversed upon in vitro antigen restimulation (Fig. 8).

Because reduced CTL activity may reflect low TCR avidity (24, 26), we investigated whether acutely infected C3H/HeN and CBA/J neonates generate MT389-specific CD8^{+} T cells differing in TCR avidity. Spleen cells from 13-d-old newborn inoculated C3H/HeN and CBA/J mice, the age for peak expansion of MT389-specific CD8^{+} T cells in infected neonates of each strain, were stimulated with graded doses of antigenic peptide for 5 h, then stained for intracellular IFN-γ. Comparison of IFN-γ^{+}CD8^{+} T cell numbers at each peptide concentration as a percentage of maximal MT389 peptide stimulation revealed no major differences in functional TCR avidity by the MT389-specific CD8^{+} T cells generated in these polyoma tumor–resistant and susceptible mice (Fig. 9 A).

We then asked whether the absence of ex vivo CTL activity by MT389-specific CD8^{+} T cells in infected CBA/J neonates reflected reduced intracellular perforin levels. Repeated encounter with infected cells in vivo, such as in acutely infected CBA/J neonatal mice, could conceivably result in large-scale degranulation by antiviral CTL effectors; the consequent deficit in intracellular perforin-granzyme stores would impair ex vivo cytotoxic activity. However, Fig. 9 B shows that MT389-specific CD8^{+} T cells in newborn inoculated 13-d-old C3H/HeN and
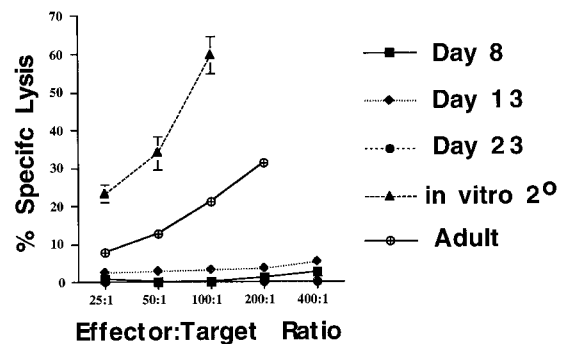

Figure 8. Kinetic analysis of ex vivo MT389-specific cytotoxic activity in newborn inoculated CBA/J mice. Spleen cells from neonatal CBA/J mice at the indicated days after infection and day 6 postinfection adult mice were assayed for lysis of ^{51}Cr-labeled syngeneic target cells pulsed with MT389 peptide (10 μM). Spleen cells from 13-d-old newborn inoculated mice were also cocultured for 5 d with polyoma-infected irradiated syngeneic spleen cells, then assayed for lysis of MT389-pulsed target cells. Each value represents the mean ± SEM percent specific lysis by spleen cells of four to five infected neonatal mice and three adult inoculated mice; results are representative of four independent experiments. No lysis of unpulsed target cells was seen by spleen cells from these infected mice at any postinfection time point, and spleen cells from naive neonatal and adult CBA/J mice did not lyse MT389 peptide-pulsed targets (data not shown).

Figure 7. Kinetic analysis of virus titers in newborn inoculated CBA/J mice. Spleens from neonatally infected mice were harvested, homogenized, and titered for polyoma virus by plaque assay. Each value represents the mean ± SD PFU/mg spleen from five to six individual mice. *, below detection limit of 1 PFU/mg.
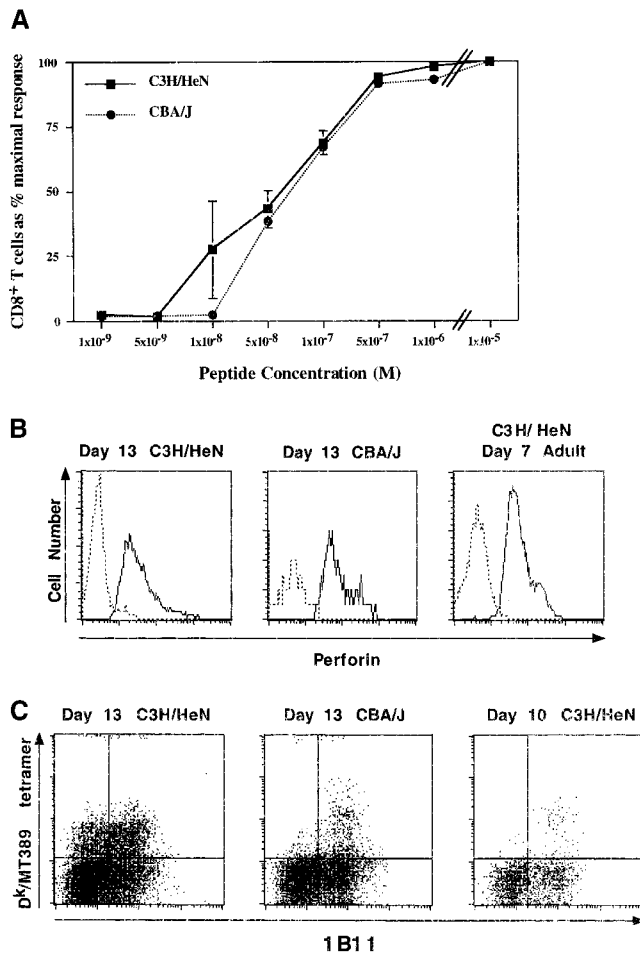
Figure 9. Comparison of TCR functional avidities and phenotypic maturation of MT389-specific CD8^{+} T cells in infected C3H/HeN and CBA/J neonatal mice. (A) Spleen cells were harvested from 13-d-old newborn inoculated mice of each strain, stimulated for 5 h with serial log dilutions of MT389 peptide, then stained for intracellular IFN-γ. The efficiency of stimulation at each peptide concentration is presented as the percentage of the number of IFN-γ^+CD8^{+} cells with respect to that at the maximal stimulating peptide dose (10 μM). Each value represents the mean $\pm$ SEM of three mice, and results are representative of two experiments. (B) Spleen cells from day 13 postinfection C3H/HeN and CBA/J neonate and day 7 postinfection C3H/HeN adult mice were surface-stained with D^k/MT389 tetramers, permeabilized, then stained for perforin and CD8. Plots are gated on D^k/MT389 tetramer^{+}CD8^{+} T cells, with dashed lines indicating staining with an isotype-matched control Ab and solid lines indicating antiperforin mAb staining. Each plot is representative of five mice. (C) Surface staining of spleen cells with D^k/MT389 tetramer, and anti-CD8α, and anti-CD43 (1B11) mAbs. Plots are gated on CD8^{+} cells, and each is representative of four to five mice.

CBA/J mice each express levels of intracellular perforin similar to those from day 7 postinfection adult C3H/HeN mice, which exhibit peak ex vivo MT389-specific cytotoxic activity (17).

Finally, we explored the possibility that MT389-specific CD8^{+} T cells in CBA/J neonates occupy a preeffector maturation stage. MT389-specific CD8^{+} T cells in both newborn inoculated C3H/HeN and CBA/J neonates nearly uniformly express upregulated surface levels of CD11a (Fig. 2 A, and data not shown), indicative of an ef-

fector/memory T cell phenotype. To distinguish between effector and memory T cells, we made use of the 1B11 mAb, which recognizes a type O-glycan epitope selectively upregulated on the cell surface of effector CD8^{+} T cells (27). As shown in Fig. 9 C, MT389-specific CD8^{+} T cells in 13-d-old infected CBA/J mice are virtually all 1B11^{hi}. D^k/MT389 tetramer^{+} cells in 13-d-old C3H/HeN neonates showed mixed 1B11 expression levels, consistent with an effector to memory T cell transition once virus is cleared (Fig. 1 B); in 10-d-old C3H/HeN neonates, when infectious virus is still detected in the spleen, most of the MT389-specific CD8^{+} T cells are 1B11^{hi}. Taken together, these findings support the conclusion that MT389-specific CD8^{+} T cells in acutely infected CBA/J neonates are cytotoxic effectors that fail to express this critical antiviral/tumor activity in vivo.

Discussion

In this study, we present quantitative in vivo evidence that neonatal mice are capable of mounting a dramatic functional antigen-specific CD8^{+} T cell response to a systemic virus infection. Using both D^k tetramers containing the immunodominant polyoma virus–specific CD8^{+} T cell epitope, MT389–397, and intracellular IFN-γ staining of MT389 peptide-stimulated T cells, we visualized massive expansion of antipolyoma CD8^{+} T cells in mice inoculated at birth to levels comparable to that of adult inoculated mice. In mice belonging to an inbred strain resistant to polyoma virus–induced tumors, this antigen-specific CD8^{+} T cell response was temporally associated with the emergence of ex vivo MT389-specific cytotoxic activity and rapid clearance of infectious polyoma virus. In contrast, mice susceptible to polyoma virus tumorigenesis cleared virus at a markedly slower rate, and, although capable of generating MT389-specific CD8^{+} T cells, these T cells exhibited a selective functional deficit in antigen–induced cytotoxic activity.

Striking similarities were observed in the MT389-specific CD8^{+} T cell response in the polyoma tumor–resistant C3H/HeN mice inoculated at birth and as adults. As a percentage of splenic CD8^{+} T cells, the peak expansion of MT389-specific CD8^{+} T cells in neonatally infected tumor–resistant mice, in fact, attained nearly twice the magnitude of that seen in adult infected mice. Consistent with our previous finding that the size of the MT389-specific CD8^{+} T cell expansion varies directly with the viral load (28), the higher level infection in newborn inoculated than adult inoculated mice is likely responsible for this larger expansion in neonatal mice. Moreover, taking into account the fact that the neonatal spleen contains <1% of the T cells of the adult spleen (29), the rate of expansion of antigen-specific CD8^{+} T cells in neonatal mice most likely exceeds that of adult mice. It is also interesting to note that there is a similar relationship between clonal burst size and size of the memory T cell pool for MT389-specific CD8^{+} T cell responses in infected adult and neonatal mice. In newborn inoculated mice, the influx of recent thymic T

cell emigrants seeding the peripheral T cell pool after viral clearance most likely accounts for the comparatively low representation of MT389-specific memory CD8^{+} T cells among the total splenic CD8^{+} T cell population; however, this peripheral seeding is not accompanied by dramatic attrition of the memory MT389-specific CD8^{+} T cell pool. MT389-specific CD8^{+} T cells in mice of both age groups also share TCR functional avidity, near matches in their TCR functional fingerprints, and nearly identical Vβ repertoires. The finding that the postinfection time point for initial detection of MT389-specific CD8^{+} T cells differed by only 2–3 d between newborn inoculated and adult inoculated mice further suggests that the MT389-specific CD8^{+} T cell response in neonatal mice resulted from the priming of T cells in newborn mice, rather than from its delayed induction by viral antigens in more mature mice.

We unexpectedly found major differences in the capacity of tetramer binding and antigen–stimulated intracellular IFN-γ production to identify polyoma-specific CD8^{+} T cells during acute infection in neonatal mice. Approximately one-third of MT389-specific CD8^{+} T cells in acutely infected neonatal mice expressed TCRs at a level apparently insufficient for stable tetramer binding, but sufficient to exceed the minimum threshold of TCR occupancy required to trigger T cell activation; these tetramer-negative T cells largely account for the discordance between tetramer and intracellular cytokine staining in detecting antigen-specific CD8^{+} T cells. Several observations favor the concept that this TCR^{low/−} population of MT389-specific CD8^{+} T cells results from TCR downmodulation, likely driven by repetitive TCR encounter with D[k]/MT389-expressing cells during acute polyoma virus infection. First, once virus is cleared, differences between tetramer binding and intracellular cytokine staining in visualizing antigen-specific CD8^{+} T cells tend to resolve. Also, in acutely infected adult mice, where peak levels of polyoma virus are 10-fold lower than in neonatal mice, these two single cell flow cytometry approaches show closer correspondence in their sensitivity for detecting MT389-specific CD8^{+} T cells (17). The possibility that neonatal mice, in contrast to adult mice, intrinsically possess TCR^{low/−} and TCR^{high}CD8^{+} T cell subpopulations is also unlikely, as no differences in α/β TCR expression by CD8^{+} T cells were seen between uninfected 13-d-old and adult C3H/HeN mice (data not shown). Although our findings implicate TCR downmodulation as the likely explanation for the inability of tetramers to stain all antigen-specific T cells, alternative mechanisms may also be operative, including the generation of antiviral CD8^{+} T cell populations during acute infection that express TCRs of weak avidity, or of a conformation or cell surface distribution unfavorable for stable tetramer binding (24, 30).

Our findings suggest that small differences in the magnitude of the antiviral CD8^{+} T cell response in the face of high viral load may determine their cytotoxic effector functionality. Mtv-7 superantigen–mediated deletion of thymocytes expressing Vβ6 and Vβ8.1, the predominant Vβ members used by MT389-specific CD8^{+} T cells in re-

sistant mice (13, 17), reduces the number of MT389-specific CD8^{+} T cell clones in the naive T cell repertoire of susceptible mice. Thus, inheritance of this endogenous Mtv provirus is likely to be a major determinant of polyoma tumor susceptibility (10). Given the considerably lower number of splenic T cells in neonatal versus adult mice (29), differences between Mtv-7^{+} and Mtv-7^{−} H-2[k] mice in the size of the precursor antipolyoma CD8^{+} T cell pool, coupled with the higher viral load in neonates, may magnify the importance of small differences in MT389-specific CD8^{+} T cell numbers in neonatally infected mice for defense against primary polyoma virus infection. It is important to point out that because the H-2[k] mice used in this study are not congenic for Mtv-7, other genetic differences may contribute to susceptibility to polyoma virus–induced tumors. In this connection, Benjamin and coworkers (31) recently reported that an H-2[k] wild-derived inbred mouse strain lacking endogenous Mtvs is susceptible to polyoma virus–induced tumors. Interestingly, the frequency of Vβ6^{+}CD8^{+} T cells in adult mice of this strain is lower than that of resistant H-2[k] inbred mice. It would be valuable to measure the magnitude of the MT389-specific CD8^{+} T cell response in infected neonatal mice of this wild-derived inbred strain and assess the integrity of its effector activities.

The absence of ex vivo cytotoxic activity by MT389-specific CD8^{+} T cells in susceptible mice clearly compromises the host's ability to control polyoma virus infection. T cell–mediated clearance of polyoma virus during acute infection is associated with protection against outgrowth of polyoma-induced tumors (32). This is easily envisioned for H-2[k] mice where the dominant antipolyoma CD8^{+} T cell response is directed towards an epitope in MT, a nonstructural viral protein whose constitutive expression is required both for efficient productive viral infection and maintenance of cellular transformation (33–35).

Several mechanisms may be invoked to account for this defect in CD8^{+} T cell cytotoxic effector function. Comparable TCR functional avidities between MT389-specific CD8^{+} T cells in resistant and susceptible mice argue against major perturbations in the TCR signaling apparatus, as reported for tumor-infiltrating and HIV-specific CD8^{+} T cells (36, 37). Partial anergy is also unlikely, as higher levels of TCR occupancy by CD8^{+} T cells are needed for triggering IFN-γ production than cytotoxic activity (38). Recent studies suggest that incomplete maturation of virus-specific CD8^{+} T cells in vivo may be responsible for impaired cytotoxic effector activity. HIV-specific CD8^{+} T cells, which exhibit weak cytotoxicity, have been shown to concomitantly express low perforin levels and a pattern of surface maturation markers suggestive of immature effector cells (39). In addition, Spencer and Braciale (30) recently described an influenza virus–specific memory CD8^{+} T cell population requiring multiple rounds of in vitro antigen stimulation to promote their differentiation into CTL effectors. However, two lines of evidence argue against incomplete differentiation of polyoma-specific CD8^{+} T cells in susceptible mice as an explanation for their lack of cytotoxic activity. First, MT389-specific CD8^{+} T cells from re-

sistant and susceptible mice express similar levels of perforin. Second, MT389-specific CD8$^+$ T cells in resistant and susceptible mice exhibit upregulated expression of cell surface O-glycans, a phenotype tightly associated with CTL activity (27). Taken together, these findings indicate that in mice susceptible to polyoma virus–induced tumors the dominant antipolyoma CD8$^+$ T cell response appears to be fully armed with, but restrained from using, its cytotoxic effector activity.

The presence of CD8$^+$ T cells partially or completely lacking antigen-triggered effector activity has been observed in persistent viral infections and cancer-bearing hosts (14, 39, 40). In these situations of chronic antigen exposure, host mechanisms may come into play to intentionally downregulate CTL activity to prevent widespread destruction of antigen-bearing cells. For persistent viruses with oncogenic potential, such as mouse polyoma virus, early termination of cytotoxic effector functionality by antiviral CD8$^+$ T cells would clearly impair immune surveillance against virus-induced neoplastic cells. Furthermore, as peak MT389-specific CD8$^+$ T cell numbers differ only fourfold between acutely infected neonatal mice having opposite polyoma tumor susceptibilities, a fine balance likely exists between the size of the initial antipolyoma CD8$^+$ T cell response and the level of infectious virus that decides the fate of CD8$^+$ T cell functional competence in vivo. Elucidation of the in vivo mechanisms that control antigen-specific CD8$^+$ T cell effector activity in the setting of persistent antigen is essential for development of immunotherapeutic strategies against viral oncogenesis.

References

1. Forsthuber, T., H.C. Yip, and P.V. Lehmann. 1996. Induction of T$_H$1 and T$_H$2 immunity in neonatal mice. *Science.* 271:1728–1730.

2. Ridge, J.P., E.J. Fuchs, and P. Matzinger. 1996. Neonatal tolerance revisited: turning on newborn T cells with dendritic cells. *Science.* 271:1723–1726.

3. Sarzotti, M., D.S. Robbins, and P.M. Hoffman. 1996. Induction of protective CTL responses in newborn mice by a murine retrovirus. *Science.* 271:1726–1728.

4. Siegrist, C.-A., F. Saddallah, C. Tougne, X. Martinez, J. Kovarik, and P.-H. Lambert. 1998. Induction of neonatal TH1 and CTL responses by live viral vaccines: a role for replication patterns within antigen presenting cells? *Vaccine.* 16:1473–1478.

5. Sarzotti, M., T.A. Dean, M.P. Remington, C.D. Ly, P.A. Furth, and D.S. Robbins. 1997. Induction of cytotoxic T cell responses in newborn mice by DNA immunization. *Vaccine.* 15:795–797.

6. Wang, Y., Z. Xiang, S. Pasquini, and H.C.J. Ertl. 1997. Immune response to neonatal genetic immunization. *Virology.* 228:278–284.

7. Hassett, D.E., J. Zhang, M. Slifka, and J.L. Whitton. 2000. Immune responses following neonatal DNA vaccination are long-lived, abundant, and qualitatively similar to those induced by conventional immunization. *J. Virol.* 74:2620–2627.

8. Pertmer, T.M., A.E. Oran, J.M. Moser, C.A. Madorin, and H.L. Robinson. 2000. DNA vaccines for influenza virus: differential effects of maternal antibody on immune responses to hemagglutinin and nucleoprotein. *J. Virol.* 74:7787–7793.

9. Freund, R., T. Dubensky, R. Bronson, A. Sotkinov, J. Carroll, and T. Benjamin. 1992. Polyoma tumorigenesis in mice: evidence for dominant resistance and dominant susceptibility genes of the host. *Virology.* 191:724–731.

10. Lukacher, A.E., Y. Ma, J.P. Carroll, S.R. Abromson-Leeman, J.C. Laning, M.E. Dorf, and T.L. Benjamin. 1995. Susceptibility to tumors induced by polyoma virus is conferred by an endogenous mouse mammary tumor virus superantigen. *J. Exp. Med.* 181:1683–1692.

11. Ting, R.C., and L.W. Law. 1965. The role of the thymus in transplantation resistance induced by polyoma virus. *J. Natl. Cancer Inst.* 34:521–527.

12. Law, L.L. 1966. Immunologic responsiveness and the induction of experimental neoplasms. *Cancer Res.* 26:1121–1132.

13. Lukacher, A.E., and C.S. Wilson. 1998. Resistance to polyoma virus-induced tumors correlates with CTL recognition of an immunodominant H-2D^k-restricted epitope in the middle T protein. *J. Immunol.* 160:1724–1734.

14. Lee, P.P., C. Yee, P.A. Savage, L. Fong, D. Brockstedt, J.S. Weber, D. Johnson, S. Swetter, J. Thompson, P.D. Greenberg, et al. 1999. Characterization of circulating T cells specific for tumor-associated antigens in melanoma patients. *Nat. Med.* 5:677–685.

15. Sogn, J.A. 1998. Tumor immunology: the glass is half full. *Immunity.* 9:757–763.

16. Letsch, A., U. Keilhalz, D. Schadendorf, D. Nagorsen, A. Schmittel, E. Thiel, and C. Scheibenbogen. 2000. High frequencies of circulating melanoma-reactive CD8$^+$ T cells in patients with advanced melanoma. *Int. J. Cancer.* 87:659–664.

17. Lukacher, A.E., J.M. Moser, A. Hadley, and J.D. Altman. 1999. Visualization of polyoma virus-specific CD8$^+$ T cells in vivo during infection and tumor rejection. *J. Immunol.* 163:3369–3378.

18. Ward, P.L., H. Koeppen, T. Hurteau, and H. Schreiber. 1989. Tumor antigens defined by cloned immunological probes are highly polymorphic and are not detected on autologous normal cells. *J. Exp. Med.* 170:217–232.

19. de Bergeyck, V., E. De Plaen, P. Chomez, T. Boon, and A. Van Pel. 1994. An intracisternal A-particle sequence codes for an antigen recognized by syngeneic cytolytic T lymphocytes on a mouse spontaneous leukemia. *Eur. J. Immunol.* 24:2203–2212.

20. Wilson, C.S., J.M. Moser, J.D. Altman, P.E. Jensen, and A.E. Lukacher. 1999. Cross-recognition of two middle T protein epitopes by immunodominant polyoma virus-specific CTL. *J. Immunol.* 162:3933–3941.

21. Murali-Krishna, K., J.D. Altman, M. Suresh, D.J. Sourdive, A.J. Zajac, J.D. Miller, J. Slansky, and R. Ahmed. 1998. Counting antigen-specific CD8 T cells: a reevaluation of bystander activation during viral infection. *Immunity.* 8:177–187.

22. Engelhard, V.H. 1994. Structure of peptides associated with MHC class I molecules. *Curr. Opin. Immunol.* 6:13–23.

23. O'Connell, K.A., and L.R. Gooding. 1984. Cloned cytotoxic T lymphocytes recognize cells expressing discrete fragments of the SV40 tumor antigen. *J. Immunol.* 132:953–958.

24. Busch, D.H., and E.G. Pamer. 1999. T cell affinity maturation by selective expansion during infection. *J. Exp. Med.* 189:701–710.

25. Savage, P.A., J.J. Boniface, and M.M. Davis. 1999. A kinetic basis for T cell receptor repertoire selection during an immune response. *Immunity.* 10:485–492.

26. Morgan, D.J., H.T. Kreuwel, S. Fleck, H.I. Levitsky, D.M. Pardoll, and L.A. Sherman. 1998. Activation of low avidity CTL specific for a self epitope results in tumor rejection but not autoimmunity. *J. Immunol.* 160:643–651.

27. Harrington, L.E., M. Galvan, L.G. Baum, J.D. Altman, and R. Ahmed. 2000. Differentiating between memory and effector CD8 T cells by altered expression of cell surface O-glycans. *J. Exp. Med.* 191:1241–1246.

28. Drake III, D.R., J.M. Moser, A. Hadley, J.D. Altman, C. Maliszewski, E. Butz, and A.E. Lukacher. 2000. Polyoma virus-infected dendritic cells induce antiviral CD8+ T lymphocytes. *J. Virol.* 74:4093–4101.

29. Piguet, P.F., C. Irle, E. Kollatte, and P. Vassalli. 1981. Post-thymic T lymphocyte maturation during ontogenesis. *J. Exp. Med.* 154:581–593.

30. Spencer, J.V., and T.J. Braciale. 2000. Incomplete CD8+ T lymphocyte differentiation as a mechanism for subdominant cytotoxic T lymphocyte responses to a viral antigen. *J. Exp. Med.* 191:1687–1698.

31. Velupillai, P., I. Yoshizawa, D.C. Dey, S.R. Nahill, J.P. Carroll, R.T. Bronson, and T.L. Benjamin. 1999. Wild-derived inbred mice have a novel basis of susceptibility to polyomavirus-induced tumors. *J. Virol.* 73:10079–10085.

32. Wirth, J.J., and M.M. Fluck. 1991. Immunological elimination of infected cells as the candidate mechanism for tumor protection in polyomavirus-infected mice. *J. Virol.* 65:6985–6988.

33. Raptis, L., H. Lamfrom, and T.L. Benjamin. 1985. Regulation of cellular phenotype and expression of polyomavirus middle T antigen in rat fibroblasts. *Mol. Cell. Biol.* 5:2476–2485.

34. Garcea, R.L., D.A. Talmage, A. Harmatz, R. Freund, and T.L. Benjamin. 1989. Separation of host range from transformation functions of the hr-t gene of polyomavirus. *Virology.* 168:312–319.

35. Freund, R., A. Sotkinov, R.T. Bronson, and T.L. Benjamin. 1992. Polyoma virus middle T is essential for virus replication and persistence as well as for tumor induction in mice. *Virology.* 191:716–723.

36. Correa, M.R., A.C. Ochoa, P. Ghosh, H. Mizoguchi, L. Harvey, and D.L. Longo. 1997. Sequential development of structural and functional alterations in T cells from tumor-bearing mice. *J. Immunol.* 158:5292–5296.

37. Trimble, L.A., P. Shankar, M. Patterson, J.P. Daily, and J. Lieberman. 2000. Human immunodeficiency virus-specific CD8 T lymphocytes have down-modulated CD3ζ and CD28, key signaling molecules for T-cell activation. *J. Virol.* 74:7320–7330.

38. Valitutti, S., S. Muller, M. Dessing, and A. Lanzavecchia. 1996. Different responses are elicited in cytotoxic T lymphocytes by different levels of T cell receptor occupancy. *J. Exp. Med.* 183:1917–1921.

39. Appay, V., D.F. Nixon, S.M. Donahoe, G.M.A. Gillespie, T. Dong, A. King, G.S. Ogg, H.M.L. Spiegal, C. Conlon, C.A. Spina, et al. 2000. HIV-specific CD8+ T cells produce antiviral cytokines but are impaired in cytolytic function. *J. Exp. Med.* 192:63–75.

40. Zajac, A.J., J.N. Blattman, K. Murali-Krishna, D.J. Sourdive, M. Suresh, J.D. Altman, and R. Ahmed. 1998. Viral immune evasion due to persistence of activated T cells without effector function. *J. Exp. Med.* 188:2205–2213.